RESEARCH LETTER

Base substitutions at scissile bond sites are sufficient to alter RNA-binding and cleavage activity of RNase III

Kyungsub Kim[1], Se-Hoon Sim[1], Che Ok Jeon[1], Younghoon Lee[2] & Kangseok Lee[1]

[1]Department of Life Sciences (BK21 program), Chung-Ang University, Seoul, Korea; and [2]Department of Chemistry, KAIST, Daejeon, Korea

Correspondence: Kangseok Lee, Department of Life Sciences (BK21 program), Chung-Ang University, Seoul 156-756, Korea. Tel.: +82 2 820 5241; fax: +82 2 825 5206; e-mail: kangseok@cau.ac.kr

Received 19 August 2010; revised 20 October 2010; accepted 17 November 2010. Final version published online 6 December 2010.

DOI:10.1111/j.1574-6968.2010.02169.x

Editor: Skorn Mongkolsuk

Keywords
bdm; rnc; endoribonuclease; RNase III.

Abstract

RNase III, a double-stranded RNA-specific endoribonuclease, degrades *bdm* mRNA via cleavage at specific sites. To better understand the mechanism of cleavage site selection by RNase III, we performed a genetic screen for sequences containing mutations at the *bdm* RNA cleavage sites that resulted in altered mRNA stability using a transcriptional *bdm′-′cat* fusion construct. While most of the isolated mutants showed the increased *bdm′-′cat* mRNA stability that resulted from the inability of RNase III to cleave the mutated sequences, one mutant sequence (wt-L) displayed *in vivo* RNA stability similar to that of the wild-type sequence. *In vivo* and *in vitro* analyses of the wt-L RNA substrate showed that it was cut only once on the RNA strand to the 5′-terminus by RNase III, while the binding constant of RNase III to this mutant substrate was moderately increased. A base substitution at the uncleaved RNase III cleavage site in wt-L mutant RNA found in another mutant lowered the RNA-binding affinity by 11-fold and abolished the hydrolysis of scissile bonds by RNase III. Our results show that base substitutions at sites forming the scissile bonds are sufficient to alter RNA cleavage as well as the binding activity of RNase III.

Introduction

In recent years, the RNase III family of enzymes has emerged as one of the most important types of endoribonuclease in the control of mRNA stability in higher organisms (Lee *et al.*, 2006; Jaskiewicz & Filipowicz, 2008; Ramachandran & Chen, 2008). In *Esherichia coli*, RNase III is one of the major enzymes in the processing and decay of RNA (Nicholson, 1999; Sim *et al.*, 2010).

Bacterial RNase III is active as a homodimer and cleaves phosphodiester bonds, creating 5′-phosphate and 3′-hydroxyl termini with a 3′-overhang of two nucleotides. *Esherichia coli* RNase III that is encoded by the *rnc* gene recognizes its substrates through specific structural and sequence features (reactivity epitopes) that are contained within a double-helical structure of at least one full turn (11 bp), a primary reactive epitope (Dunn, 1982; Robertson, 1982; Court, 1993; Nicholson, 1999, 2003). Internal loops or bulges in the helix can limit the cleavage of a target site to a single phosphodiester (Robertson, 1982; Court, 1993; Nicholson, 1999). In addition, a bulge–helix–bulge motif has been identified that allows binding of *E. coli* RNase III, but inhibits cleavage (Calin-Jageman & Nicholson, 2003). While a number of identified bacterial RNase III substrates have no sequence conservation as positive recognition determinants, it has been proposed that specific base pair sequences can be excluded from two discrete double-helical segments, termed the proximal box (pb) and the distal box (db) (Zhang & Nicholson, 1997). Introduction of one or more of the excluded base pairs into either box within a model substrate inhibits RNA binding by *E. coli* RNase III (Zhang & Nicholson, 1997). Based on these findings, it was proposed that reactive *E. coli* RNase III sites are identified by the absence of inhibitory base pairs within the pb and db (Zhang & Nicholson, 1997; Nicholson, 1999). While positive sequence recognition determinants for cleavage site selection by RNase III are not known, nonetheless, such elements may exist and may be common features of the diverse substrates for bacterial RNases III, which have not yet been discovered.

In this study, to investigate determinants for cleavage site selection by RNase III, we performed a genetic screen for mutant sequences at the RNase III cleavage sites present in *bdm* mRNA that resulted in altered RNase III cleavage activity using a transcriptional *bdm′-′cat* fusion construct

FEMS MICROBIOLOGY LETTERS

(Sim *et al.*, 2010). Based on analyses of the isolated mutant sequences that altered RNase III cleavage activity, we show that base compositions at scissile bond sites play an important role in both RNA-binding and cleavage activity of RNase III, which may explain the ability of bacterial RNase III to carry out site-specific cleavage of cellular RNA substrates despite its ability to degrade long double-stranded RNAs of broad sequence into short duplex products in a largely base pair sequence-independent manner under *in vitro* conditions (Xiao *et al.*, 2009).

Materials and methods

Introduction of random mutations at the RNase III cleavages sites in *bdm* mRNA

DNA fragments containing random mutations at the cleavages sites 3 and 4-II in *bdm* mRNA (Sim *et al.*, 2010) were amplified using overlap extension PCR, were digested with NcoI and NotI, and were cloned into the same sites in pBRS1 (Sim *et al.*, 2010). The primers used were bdm-reporter 1 (5′-GCATAGCGGCCGCTTTATAAATCTGCGATCCGTA), bdm-reporter 2 (5′-CCTTGTCGCCTTGCGTATAA), bdm-reporter 3 (5′-AGAAGCTTCAACCCATTTGGTCAGCTC CATGAGAATGTCATCNNCAGTGACAACACCATGCTGT), and bdm-reporter 4 (5′-CCAAATGGGTTGAAGCTTCTGA TAACGACATCCTNNGTGATATCTACCAGCAAACG).

Minimum inhibitory concentration (MIC) and Western blot analysis

MICs were determined as described previously (Sim *et al.*, 2010). Western blot analysis of the chloramphenicol acetyl transferase (CAT) protein was performed as described previously (Kim *et al.*, 2009).

Real-time PCR analysis

To measure steady-state levels of mutant *bdm′-′cat* mRNA, cDNA was synthesized using a Prime Script first-strand cDNA synthesis kit (Takara) using 1 μg of total RNA isolated from *E. coli* cells expressing mutant *bdm′-′cat* mRNA as a template. Then, real-time PCR was performed in a C1000 Thermal Cycler (BioRad) using SYBR Premix Ex Taq (Takara) with the synthesized cDNA as a template. The primers used were: 5′-ATGTTTACTTATTATCAGGCAG and 5′-TTAAAGCGTAGGGTGCTGGCCAC for *bdm*, 5′-TG ACGAAGTTGACGTTGCTC and 5′-CTTCCAGGTGCAGA GTGTCA for *rpsA*.

Primer extension analysis and *in vitro* RNA cleavage

Both a primer extension analysis and an *in vitro* RNA cleavage assay were performed as described previously (Sim *et al.*, 2010). In this study, bdm loop RNA transcripts were synthesized using PCR DNA as a template. PCR DNA was synthesized using two primers, T7 bdm loop F (5′-TAA TACGACTCACTATAGGGGCATGGTGTTGTCACTG) and bdm +175R (5′-TTGCTGGTAGATATCAC), and the template DNA was pBRS1 or pBRS1, which contained mutations at the RNase III cleavage sites. Synthesized bdm loop RNA transcripts were either 5′-end labeled with [γ-^{32}P]ATP (3000 mCi mmol^{-1}) and T4 polynucleotide kinase (Takara) or 3′-end labeled with [5′-^{32}P]pCp (3000 mCi mmol^{-1}) and T4 RNA ligase (New England Biolab), separated in 4% polyacrylamide gels containing 8 M urea. The transcripts were eluted from the gel via mixing in a buffer containing 30 mM Tris-HCl, pH 7.9, 10 mM NaCl, 0.1% sodium dodecyl sulfate, and 0.1 mM EDTA, pH 8.0, for 16 h and were purified using phenol–chloroform extraction and ethanol precipitation. His-tagged RNase III purification and cleavage assays were performed as described previously (Amarasinghe *et al.*, 2001). Briefly, 1 pmol of labeled RNA was incubated with 0.5 μg of purified RNase III in the presence of 0.25 μg mL^{-1} of yeast tRNA (Ambion) and 20 U of RNaseOUT^{TM} (Takara) in cleavage buffer (30 mM Tris-HCl, pH 7.9, 160 mM NaCl, 0.1 mM dithiothreitol, 0.1 mM EDTA, pH 8.0). Cleavage reactions were initiated by adding 10 mM $MgCl_2$ after 5 min of incubation at 37 °C. Samples were removed at the designated time intervals, mixed with an equal volume of Gel Loading Buffer II (Ambion), denatured at 65 °C for 10 min, and separated on an 8% polyacrylamide gel containing 8 M urea.

Electrophoretic mobility shift assay (EMSA)

EMSAs were performed as described previously (Pertzev & Nicholson, 2006). In these assays, Mg^{2+} was replaced by Ca^{2+}, promoting substrate binding to RNase III while preventing substrate cleavage. Briefly, 5′-end-labeled RNA was incubated at 37 °C for 10 min with RNase III in a buffer containing 30 mM Tris-HCl, pH 8.0, 160 mM NaCl, 10 mM $CaCl_2$, 0.1 mM EDTA, 0.1 mM dithiothreitol, 5% glycerol, and yeast tRNA (5 μg mL^{-1}). The binding reactions were placed on ice for 20 min and then electrophoresed (6 V cm^{-1}) at 4 °C in a 10% nondenaturing polyacrylamide gel (80 : 1 acrylamide : bisacrylamide) containing 0.5 × TBE buffer and 10 mM $CaCl_2$. Binding reactions were visualized using PHOSPHORIMAGING and were quantified using IMAGEQUANT software.

Results

Isolation of RNase III cleavage site mutants

A previous study has shown that RNase III cleaves *bdm* mRNA at specific sites (Fig. 1a) and consequently controls its stability (Sim *et al.*, 2010). This *in vivo* RNase III substrate

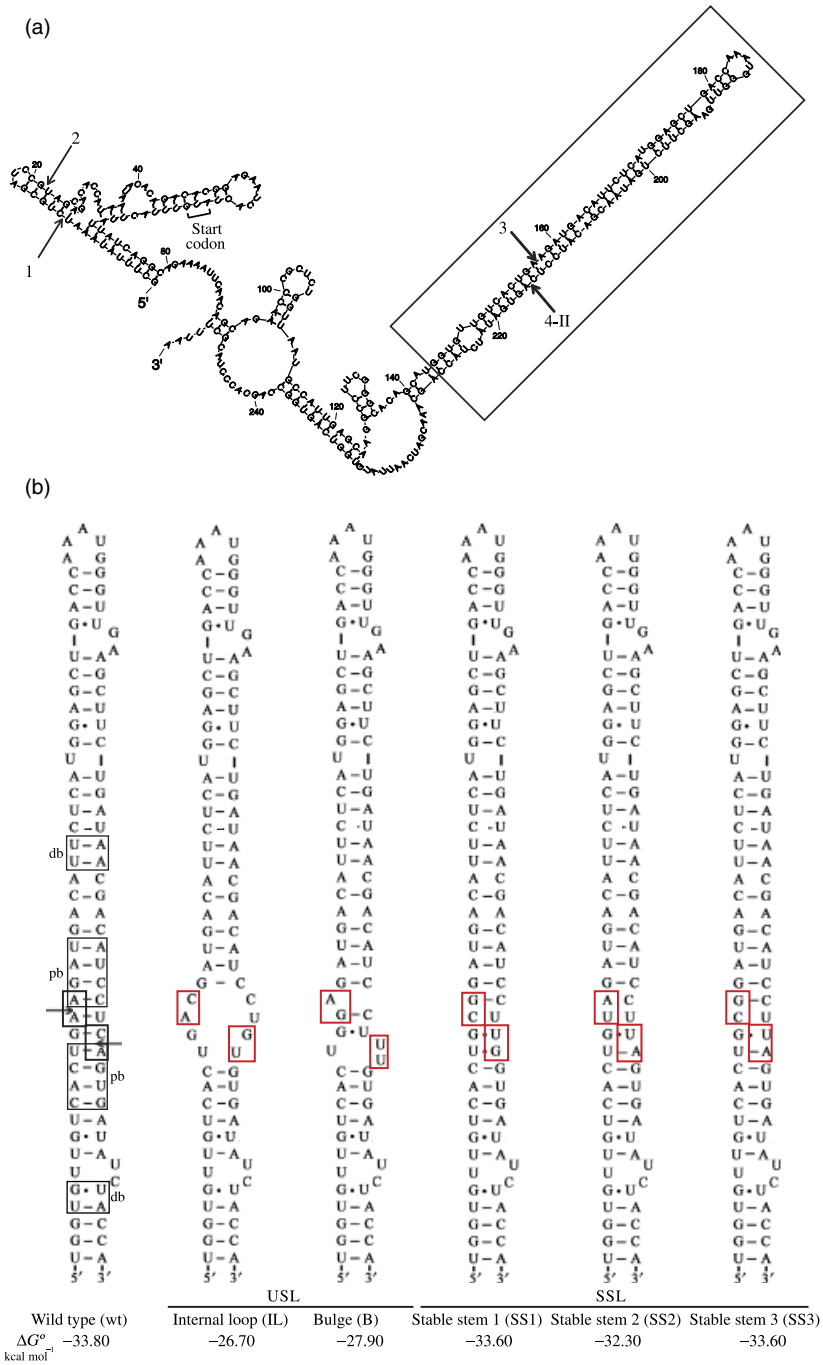

Fig. 1. Isolation of the *bdm′-′cat* mRNA variants with mutations at the RNase III cleavage site. (a) Predicted secondary structure of *bdm* mRNA. The RNase III cleavage sites (1–3 and 4-II) identified by Sim *et al*. (2010) and the start codon are shown. The hairpin within the box was used for analyses in (b) and for *in vitro* synthesis of *bdm* loop transcripts in Fig. 3. (b) Secondary structures and free energy values (ΔG°) of the region encompassing the RNase III cleavage sites in *bdm′-′cat* mRNAs were predicted using the M-FOLD program. Domains affecting the recognition and binding of RNase III to target RNA, db and pb, were assigned according to the criteria of Zhang & Nicholson (1997). The nucleotides within the red rectangles refer to the mutated nucleotides and the arrows indicate the RNase III cleavage sites.

was utilized to investigate the roles of nucleotides that compose scissile bonds in the selection and cleavage of target RNA by RNase III. We introduced nucleotide substitutions at the RNase III cleavage sites 3 and 4-II in a transcriptional *bdm′-′cat* fusion mRNA (Fig. 1b) and screened for clones that showed increased or wild-type-like degrees of resistance to chloramphenicol. The transcriptional *bdm′-′cat* fusion construct expresses mRNA containing a 5′-untranslated region and the coding region of *bdm* that are fused to the coding region of CAT (Sim *et al*., 2010). The fusion mRNA was constitutively expressed from a mutant tryptophan promoter (Lee *et al*., 2001) in a multicopy plasmid (pBRS1). Sixty-seven mutant sequences were obtained and were classified into two groups based on

Table 1. Analysis of *bdm* loop mutants*

	SSL		USL	
Group				
Secondary structure	Wild type	Stable stem	Internal loop	Bulge
ΔG° (kcal mol^{-1})†	− 33.80	− 32.09	− 27.55	− 28.31
Number of clones	NA	25	30	12

**bdm′-′cat* mutants were analyzed using the secondary structures predicted by the M-FOLD program and were grouped as indicated.
†Free energy is the mean value of the mutants in each group.
NA, not applicable.

secondary structures and the stability of hairpins containing the RNase III cleavage sites 3 and 4-II that were predicted by the M-FOLD program (Table 1, Fig. 1b, and Supporting Information, Table S1). Forty-two sequences were classified into the unstable stem loop (USL) group and were predicted to contain an internal loop or bulges with free energy of formation of secondary structures higher than that of a wild-type sequence (− 33.8 kcal mol^{-1}). The rest of the sequences were predicted to form stable stem structures with a free energy similar to that of the wild-type sequence and were referred to as stable stem loop (SSL) mutants. Expression of mutant *bdm′-′cat* fusion mRNA in the USL group resulted in increased resistance of the cells to chloramphenicol compared with that of the cells expressing *bdm′-′cat* fusion mRNA containing a wild-type sequence, indicating the existence of an internal loop or bulge at the cleavage site that can act as a negative determinant of RNase III activity (Fig. 2a). However, only one mutant sequence in the SSL group exhibited a wild-type-like phenotype in terms of degree of resistance to chloramphenicol, while other mutants in the group showed a higher degree of resistance

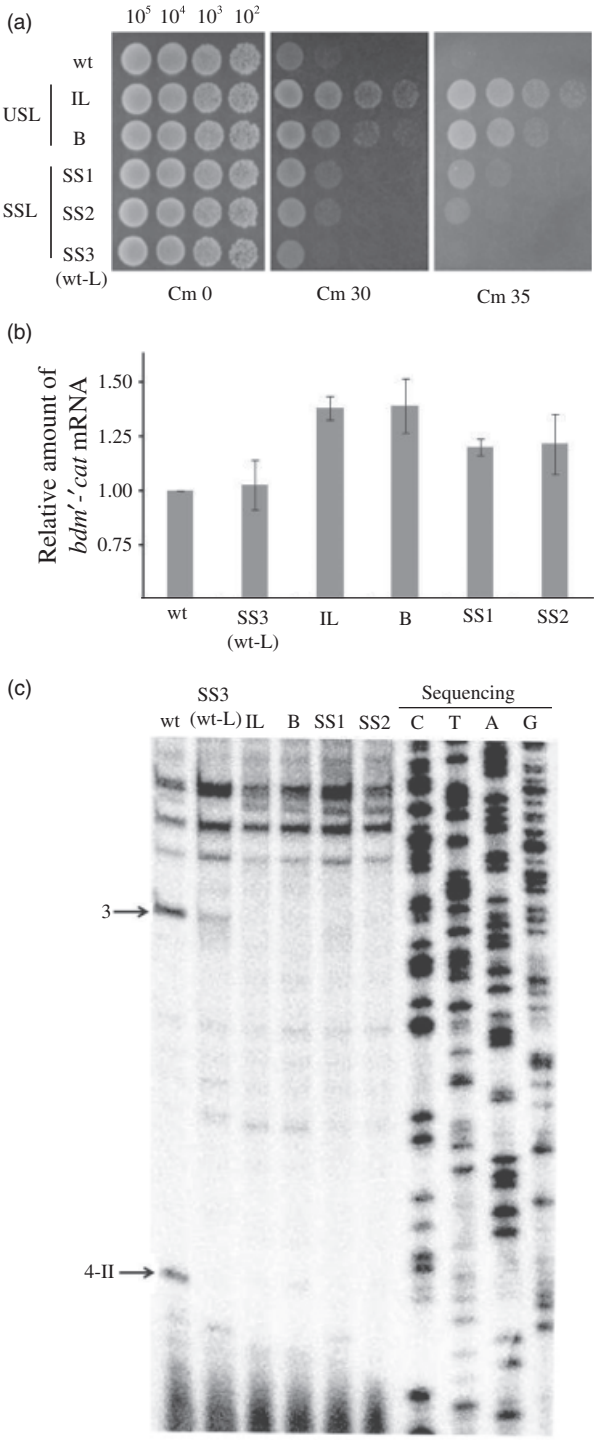

Fig. 2. *In vivo* analyses of the isolated *bdm′-′cat* mutants. (a) Effects of mutations at the RNase III cleavage sites on *bdm′-′cat* mRNA activity. W3110 cells expressing the wild-type or mutant *bdm′-′cat* mRNA were grown to the mid-log phase ($OD_{600\,nm}$ = 0.6–0.8) and individually tested on Luria–Bertani agar medium containing 0–35 μg mL^{-1} of chloramphenicol. The approximate number of cells in a spot is shown at the top of figure in the left panel. (b) Effects of mutations at the RNase III cleavage sites on steady-state levels of *bdm′-′cat* mRNA. Steady-state levels of *bdm′-′cat* mRNA were measured using real-time PCR. The relative abundance of *bdm′-′cat* mRNA were measured by setting the amount of *bdm′-′cat* mRNA in W3110 cells expressing wild-type *bdm′-′cat* mRNA to one. Levels of *rpsA* mRNA, which were independent of the cellular concentrations of RNase III (Sim *et al.*, 2010), were used to normalize the amount of *bdm′-′cat* mRNA. (c) Effects of mutations at the RNase III cleavage sites on RNase III cleavage activity. RNase III cleavage products of *bdm′-′cat* mRNA were analyzed by extending the 5′-end-labeled primer (bdm+200R) using Avian Myeloblastosis Virus (AMV) reverse transcriptase with total RNA as a template. Synthesized cDNA products were analyzed in an 8% polyacrylamide gel containing 8 M urea. Sequencing ladders (C, T, A, and G) were produced using the same primer as in cDNA synthesis and PCR DNA encompassing the coding sequence (CDS) of *bdm* mRNA as a template. The extra bands near the top of the gel are premature cDNA products. The arrows indicate the RNase III cleavage sites 3 and 4-II. The abbreviations used for *bdm′-′cat* mRNA variants are shown in Fig. 1b.

to chloramphenicol compared with that of the wild type. These results imply that most of the mutant sequences that form stable stem structures may not react with RNase III as efficiently as does the wild-type sequence.

Measurement of RNase III cleavage activity on *bdm′-′cat* mRNA *in vivo*

To test whether the activity of mutant *bdm′-′cat* mRNA is related to the RNase III cleavage activity on the mutant sequences, *in vivo* steady-state levels of two mutant sequences from each group along with a wild-type sequence were analyzed. Total RNA was isolated from the cells and used for real-time PCR analysis. Steady-state levels of mutant *bdm′-′cat* mRNAs that resulted in the enhanced resistance to chloramphenicol were increased by approximately 1.5–2.0-fold compared with those of the wild-type sequence (Fig. 2b). However, steady-state levels of the mutant wt-L that showed a wild-type-like phenotype were similar to those of the wild-type sequence, indicating that the mutant wt-L mRNA is processed by RNase III. We further investigated RNase III cleavage activity on these mutant sequences via primer extension analyses (Fig. 2c). Mutant sequences that resulted in a higher degree of resistance to chloramphenicol were not cleaved by RNase III, while the mutant sequence (wt-L) that showed a wild-type-like phenotype was mainly cut only once at cleavage site 3, located to the 5′-terminus of the stem loop. Interestingly, we found that a base substitution at the RNase III cleavage site on the RNA strand to the 3′-terminus in wt-L mutant RNA in one of mutants tested here (SSL-1) abolished RNase III cleavage activity at both target sites.

In vitro RNase III cleavage activity on a model hairpin RNA derived from *bdm* mRNA and its derivatives

To further characterize the molecular basis of RNase III cleavage on *bdm* mRNA, we synthesized a model hairpin RNA (bdm hp-wt) that has a nucleotide sequence between +84 and +170 nt from the start codon of *bdm*, encompassing RNase III cleavage sites 3 and 4-II in *bdm* mRNA (Fig. 1a) and used for biochemical analyses *in vitro*. Two additional mutant bdm hairpin RNA transcripts that contained mutations at the RNase III cleavage sites derived from wt-L and SSL-1 *bdm′-′cat* mRNA (bdm-hp-wt-L and bdm-hp-SSL-1, respectively) were also synthesized for comparison.

Incubation of the 5′-end-labeled bdm-hp-wt transcript with purified RNase III generated two major RNA fragments that corresponded to cleavage sites 3 and 4-II, while the bdm-hp-wt-L transcript was predominantly cleaved at the cleavage site 3 and bdm-hp-SSL-1 was not cleaved (Fig. 3a). These results confirmed the results of primer extension analyses on *in vivo bdm′-′cat* mRNA. Interestingly, RNase III cleavage of the bdm-hp-wt transcript with a radiolabeled 3′-end yielded the major cleavage product generated from the cleavage at 4-II, indicating that a majority of the initial cleavages of bdm-hp-wt transcripts by RNase III occur at the site 4-II, and this decay intermediate is further cleaved at site 3 (Fig. 3b). A similar result, albeit less dramatic, was observed in the *in vivo* analysis of wild-type *bdm′-′cat* mRNA, which showed the synthesis of more cDNAs from the *bdm* mRNA cleavage products generated by RNase III cleavage at site 4-II. RNase III cleavage of the 3′-end-labeled bdm-hp-wt-L transcript produced the major cleavage product generated from the cleavage at site 3 (Fig. 3b).

In vitro efficiency of RNase III binding to the bdm-hp-wt transcript and its derivatives

To test whether the altered RNase III cleavage activities on bdm-hp-wt and its derivatives are related to its RNA-binding activity, an EMSA was performed. One major band corresponding to the RNase III–RNA complex was observed when lower concentrations of RNase III (20 and 40 nM) were reacted with RNA (indicated as A in Fig. 3c), while another minor, fast-migrating band appeared in the reactions that contained higher concentrations of RNase III (60 and 80 nM) and RNA (indicated as B in Fig. 3c). The minor band appeared with an intensity similar to that of the major band in a manner independent of RNase III concentrations when RNase III was reacted with bdm-hp-SS1. These results indicate that the fast-migrating band may represent a loose complex or a complex formed by a monomer of RNase III and RNA. When bands A and B were considered as RNase III–RNA complex, RNase III was able to bind bdm-hp-wt and bdm-hp-wt-L in a manner dependent on the RNase III concentration with binding constants of 13.1 and 26.4 nM, respectively, while the binding constant of bdm-hp-SSL-1 was > 11 times greater than that of bdm-hp-wt (Fig. 3c). These results indicate that the inability of RNase III to cleave bdm-hp-SSL-1 stems from its poor binding to RNA.

Discussion

In this study, we demonstrated that base compositions at scissile bond sites in RNA substrate play an important role in RNA cleavage and the binding activity of RNase III. While previous studies have focused on negative determinants for RNA selection and cleavage by RNase III using mutational analyses of several RNA-binding sites outside the cleavage sites in a model RNA substrate *in vitro* (Pertzev & Nicholson, 2006), our study provides *in vivo* evidence for the existence of determinants for RNase III cleavage activity at the cleavage sites. Our *in vitro* analyses on model hairpin RNA derived from *bdm* mRNA confirmed the *in vivo* results and further identified the basis for the inability of RNase III

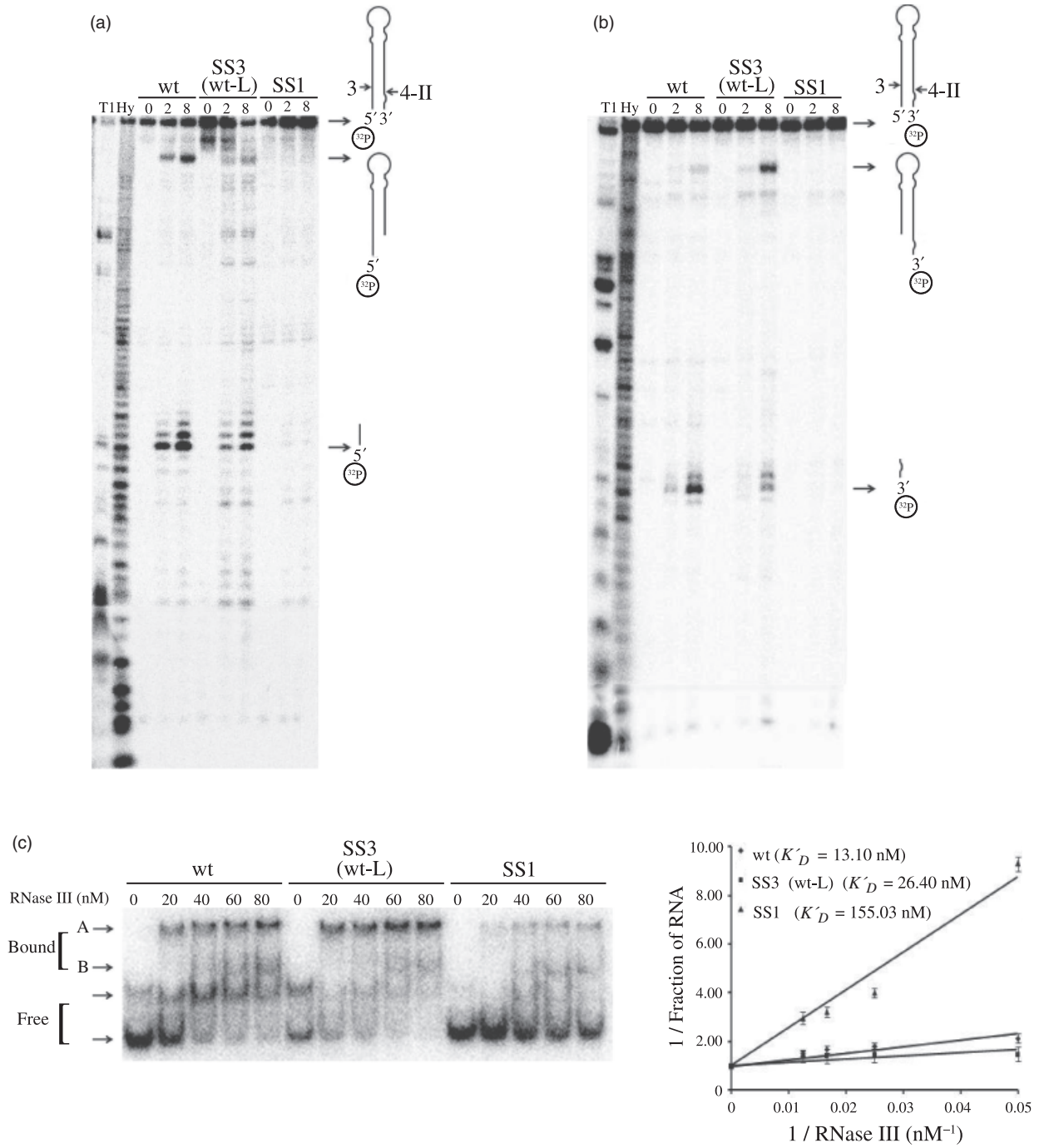

Fig. 3. *In vitro* analyses of *bdm* loop transcripts. (a, b) Effects of mutations at the RNase III cleavage sites on RNase III cleavage activity. One picomole of 5′-end-labeled (a) or 3′-end-labeled (b) *bdm* loop RNA were incubated with 0.5 μg of purified RNase III in cleavage buffer with (III+Mg^{2+}) or without $MgCl_2$ (III). Samples were withdrawn at the indicated time intervals and analyzed in a 10% polyacrylamide gel containing 8 M urea. Products from RNase T1 cleavage (T1) and alkaline hydrolysis (Hy) of the wild-type *bdm* loop RNA were loaded in the first and second lanes, respectively. (c) Effects of mutations at the RNase III cleavage sites on RNase III-binding activity. 5′-End-labeled *bdm* loop RNA was mixed with different concentrations of RNase III (0, 20, 40, 60, and 80 μM) and analyzed in a 10% polyacrylamide gel. Dissociation constants (K'_D) were calculated from the plots in the graph with SEs (right panel), which represent the average of three experiments. We obtained the K'_D from a slope that represents a linear relation between the reciprocal of the fraction of RNA bound and the reciprocal of the RNase III concentrations. The arrows indicate free and bound RNA. Two kinds of shifted RNA bands are indicated as A and B. The abbreviations used for *bdm′-′cat* mRNA variants are shown in Fig. 1b.

to cleave a mutant of the model hairpin RNA (bdm-hp-SSL-1).

A current model for RNase III action suggests a stepwise cleavage of double-stranded RNA by a coordinated action of two catalytic sites formed by RNase III dimers, which requires residues from one subunit for the selection of the scissile bond and from the partner subunit for the cleavage chemistry (Gan *et al.*, 2008). Isolation of an *in vivo* substrate that can bind RNase III as efficiently as the wild-type *bdm* mRNA, but that can be cleaved at one scissile bond indicates that a subtle change in the structures of scissile bonds can perturb the coordinated action of the two catalytic sites of RNase III. In addition, the creation of an *in vivo* mRNA substrate that can be predominantly cleaved only once and results in RNA stability similar to that of mRNA substrate cleaved at both strands raises a question of why RNase III family enzymes evolved to cleave both strands in a double-stranded region of target RNA substrates. One obvious answer is that, for the processing of structure RNAs such as rRNA transcripts and mRNAs, it is more efficient to process both RNA transcripts ends at the same time. The same reason may be applicable to the creation of microRNAs and siRNAs in higher organisms. This well-conserved mode of RNase III action might still be used to cleave cellular mRNA for degradation. Another possibility is that the cleavage products having a stem-loop structure with a 2 nt 3′-overhang in bacteria might have an undiscovered function in biological processes such as siRNA-like functions. The discovery of small RNA species that are involved in many bacterial regulatory processes (Repolia & Gottesman, 2003; Gottesman *et al.*, 2006; Marles-Wright & Lewis, 2007) supports this possibility. Further studies on RNA products resulting from the RNase III cleavage of mRNA are needed to address this possibility.

Acknowledgement

This research was supported by grants from the National Research Foundation of Korea (NRF-2009-0065181 and NRF-2010-0029167).

Authors' contribution

K.K. and S.-H.S. equally contributed to this work.

References

Amarasinghe AK, Calin-Jageman I, Harmouch A, Sun W & Nicholson AW (2001) *Escherichia coli* ribonuclease III: affinity purification of hexahistidine-tagged enzyme and assays for substrate binding and cleavage. *Method Enzymol* **342**: 143–158.

Calin-Jageman I & Nicholson AW (2003) Mutational analysis of an RNA internal loop as a reactivity epitope for *Escherichia coli* ribonuclease III substrates. *Biochemistry* **42**: 5025–5034.

Court DL (1993) RNA processing and degradation by RNase III. *Control of Messenger RNA Stability* (Belasco JG & Brawerman G, eds), pp. 71–116. Academic Press, New York.

Dunn JJ (1982) Ribonuclease III. *The Enzymes* (Boyer PD, ed), pp. 485–499. Academic Press, New York.

Gan J, Shaw G, Tropea JE, Waugh DS, Court DL & Ji X (2008) A stepwise model for double-stranded RNA processing by ribonuclease III. *Mol Microbiol* **67**: 143–154.

Gottesman S, McCullen CA, Guillier M, Vanderpool CK, Majdalani N, Benhammou J, Thompson KM, FitzGerald PC, Sowa NA & FitzGerald DJ (2006) Small RNA regulators and the bacterial response to stress. *Cold Spring Harb Sym* **71**: 1–11.

Jaskiewicz L & Filipowicz W (2008) Role of Dicer in posttranscriptional RNA silencing. *Curr Top Microbiol* **320**: 77–97.

Kim HM, Ryou SM, Song WS *et al.* (2009) Genetic analysis of the invariant residue G791 in *Escherichia coli* 16S rRNA implicates RelA in ribosome function. *J Bacteriol* **191**: 2042–2050.

Lee K, Holland-Staley CA & Cunningham PR (2001) Genetic approaches to studying protein synthesis: effects of mutations at Ψ516 and A535 in *Escherichia coli* 16S rRNA. *J Nutr* **131**: 2994S–3004S.

Lee Y, Han J, Yeom KH, Jin H & Kim VN (2006) Drosha in primary microRNA processing. *Cold Spring Harb Sym* **71**: 51–57.

Marles-Wright J & Lewis RJ (2007) Stress responses of bacteria. *Curr Opin Struc Biol* **17**: 755–760.

Nicholson AW (1999) Function, mechanism and regulation of bacterial ribonucleases. *FEMS Microbiol Rev* **23**: 371–390.

Nicholson AW (2003) The ribonuclease III superfamily: forms and functions in RNA maturation, decay, and gene silencing. *RNAi: A Guide to Gene Silencing* (Hannon GJ, ed), pp. 149–174. Cold Spring Harbor Laboratory Press, Cold Spring Harbor, NY.

Pertzev AV & Nicholson AW (2006) Characterization of RNA sequence determinants and antideterminants of processing reactivity for a minimal substrate of *Escherichia coli* ribonuclease III. *Nucleic Acids Res* **34**: 3708–3721.

Ramachandran V & Chen X (2008) Small RNA metabolism in *Arabidopsis*. *Trends Plant Sci* **13**: 368–374.

Repolia F & Gottesman S (2003) Temperature sensing by the dsrA promoter. *J Bacteriol* **185**: 6609–6614.

Robertson HD (1982) *Escherichia coli* ribonuclease III cleavage sites. *Cell* **30**: 669–672.

Sim SH, Yeom JH, Shin C *et al.* (2010) *Escherichia coli* ribonuclease III activity is downregulated by osmotic stress: consequences for the degradation of bdm mRNA in biofilm formation. *Mol Microbiol* **75**: 413–425.

Xiao J, Feehery CE, Tzertzinis G & Maina CV (2009) *E. coli* RNase III (E38A) generates discrete-sized products from long dsRNA. *RNA* **15**: 984–991.

Zhang K & Nicholson AW (1997) Regulation of ribonuclease III processing by double-helical sequence antideterminants. *P Natl Acad Sci USA* **94**: 13437–13441.

Supporting Information

Additional Supporting Information may be found in the online version of this article:

Table S1. Analysis of *bdm* loop mutants.

Please note: Wiley-Blackwell is not responsible for the content or functionality of any supporting materials supplied by the authors. Any queries (other than missing material) should be directed to the corresponding author for the article.